Role of water on the structure of palladium for methane complete oxidation

Xiansheng Li[a,b], Xing Wang[a,b], Kanak Roy[a], Jeroen A. van Bokhoven*[,a,b], Luca Artiglia*[,b,c]

[a]Institute for Chemical and Bioengineering, Department of Chemistry and Applied Biosciences, ETH Zurich, 8093 Zurich, Switzerland

[b]Laboratory for Catalysis and Sustainable Chemistry, Paul Scherrer Institut, 5232 Villigen, Switzerland

[c]Laboratory of Environmental Chemistry, Paul Scherrer Institut, 5232 Villigen, Switzerland

Abstract

Palladium-based catalysts are attractive for methane combustion on natural gas vehicles at low temperature. By means of ambient pressure x-ray photoelectron spectroscopy, we investigated the reaction on a palladium foil exposed to different mixtures at increasing temperature. Water affects the long-term catalyst stability and blocks the active sites, ascribed to the hydroxyl inhibition effect. We investigated such an effect both under steady state and under transient reaction conditions, to understand the mechanism of inhibition. The hydroxyl formation on the surface of palladium blocks the sites for methane activation, postponing the formation of the active palladium oxide phase in the bulk.

Keywords

Methane oxidation, palladium, water inhibiting, active sites, ambient pressure X-ray photoelectron spectroscopy (APXPS)

1. Introduction

Natural gas has enormous potential as an alternative to traditional automotive fuels, because of its high energy density and low emission of gaseous pollutants [1-2]. Lean-burning natural gas vehicles (NGVs) have higher fuel combustion efficiencies and minimize emissions of incomplete combustion products such as carbon monoxide and volatile organic compounds[3]. However, the fraction of unburned methane in the exhaust gas poses a great potential threat to the environment due to its strong greenhouse effect [4]. Complete methane oxidation is the main treatment technology in a NGV, however it is challenging due to the following reasons: (i)strong carbon to hydrogen bond[5], (ii)low exhaust gas temperature of NGVs[6-7] and (iii)high concentration of water in the exhaust gas[8-10].

Palladium-based catalysts are the most-active for methane complete oxidation and have been extensively investigated[8, 11-16]. It is now generally agreed that palladium oxide is the key active phase for the exceptional performance of supported palladium catalysts [6, 8, 14]. However, open questions remain, such as what is or are the role(s) of bulk vs surface palladium oxide and how does water inhibit the reaction[3, 15, 17-20]. Bruch[21] reported that the fully oxidized palladium (II) oxide is the optimum phase for methane oxidation and the intermediate state corresponding to a 'skin' of palladium oxide (surface palladium oxide) on a palladium metal core has lower activity. Fujimoto et al.[14] proposed that C-H bond activation takes place on a surface active site pair consisting of oxygen atoms and coordinatively unsaturated palladium sites. Methane from the gas phase adsorbs on the latter, while neighboring oxygen atoms extract protons from it forming hydroxyl groups. Such palladium active sites were introduced into the reaction sequence by postulating the presence of oxygen vacancies; oxygen vacancies are regenerated at the end of a catalytic cycle by recombination of surface hydroxyl groups

formed in C-H bond activation steps, which allows explaining the negative reaction order of water (equation 1). Recently, PdO_x and $Pd–PdO_x$ structures were also found on Al_2O_3-decorated Pd/SiO_2 catalysts synthesized by means of atomic layer deposition[22].

In practical applications, water significantly suppresses the activity of palladium catalysts at lower temperatures. As described in the methane oxidation kinetic rate equation,

$$r = k\,(CH_4)^{0.7}\,(O_2)^{0.2}\,(H_2O)^{-0.9}, \quad (1)$$

methane oxidation rates (calculated over a palladium foil) are inversely proportional to the concentration of water, whether water is generated during reaction or is introduced to the reaction gas mixture. The same reaction kinetic rate equation has also been evaluated on supported palladium nanoparticles catalysts, and the reaction order of water ranged from -0.9 to -1.1[13-14, 23].

So far, there have been different interpretations of the inhibitory effects of water on methane oxidation, and a clear explanation of it is still missing [6, 10, 24-26]. It was initially reported that the formation of stable and inactive surface hydroxide, $Pd(OH)_2$, inhibited and deactivated supported palladium catalysts [8, 12]. Recently, Barrett et al. observerd palladium hydroxide phase formation by means of in situ x-ray absorption spectroscopy (XAS) over Pd/Al_2O_3 catalyst[27]. They also showed that water inhibits the oxidation of metallic palladium, which is supported by temperature programmed oxidation (TPO) experiments[28] and electron microscopy[29]. However, several researchers claimed that the water inhibition is due to coverage effects, rather than structural and/or phase changes[20, 30]. The hydroxylation of the support and especially of palladium oxide by water dissociation was observed in situ by means of DRIFTS[31], and was further confirmed by other literature reports[10, 14, 26, 32]. The occupation

of coordinatively unsaturated palladium sites by water/hydroxyls is likely to inhibit methane activation on palladium oxide[24]. A considerable number of papers have demonstrated that the addition of platinum to a palladium catalyst increases the methane oxidation activity, especially under wet feed conditions.[33-35] Platinum was proposed to provide new sites for methane dissociation when palladium sites are blocked by water[34]. Additionally, suppression of oxygen exchange[26, 28, 36] was also considered as the water inhibition effect.

In general, the disagreement on the water inhibition effect in the combustion of methane could be partially assigned to the complexity of the investigated catalytic systems. The particle size, support interaction, crystal structure and activation strategy could affect the catalytic process, thus the state and behavior of active sites[37]. However, limited by the inability to directly observe oxygen and palladium at the same time, the role and behavior of surface water species for palladium species is not directly supported by experimental methods. A suitable approach would envisage the characterization of the catalyst-reactant mixture (solid-gas) interface performed in situ. The approach proposed in the present study was to use a model system to study particular aspects of the catalytic combustion chemistry of methane on palladium catalysts. Spectroscopic methods are particularly useful to investigate catalytic systems under in situ and operando conditions[38-40]. The possibility of working under reaction-relevant conditions while acquiring the spectroscopic fingerprint or the species involved has helped to identify more in depth previously unknown reaction mechanisms and to develop novel materials. Among all the in situ spectroscopic methods, ambient pressure x-ray photoelectron spectroscopy (APXPS) stands out for its surface sensitivity, which allows the direct characterization of relevant interfaces, such as the solid-gas, the liquid-vapor and the solid-liquid[41-46]. In this study, we employed in situ XPS to detect the structural development

of palladium catalysts during the oxidation of methane and to study the influence of water. Based on the experimental results, we propose that hydroxyl accumulation on the surface of palladium hinders the catalytic combustion reaction by occupying the coordinatively unsaturated palladium sites and the neighbor oxidic sites, which are the methane adsorption and activation sites. Moreover, such inhibition effect also hinders oxygen activation and mobility, preventing the formation of the bulk palladium oxide.

2. Experimental Methods

The experiments were carried out at the X07DB In Situ Spectroscopy beamline of the Swiss Light Source synchrotron. The solid-gas interface endstation, connected to a differentially pumped Scienta R4000 HiPP-2 electron analyzer, allows the manipulation of solid samples while dosing a gas/gas mixture in the mbar range. Thanks to the small volume of the experimental cell, both steady state experiments and transient state experiments are possible[47]. In the former case, a gas/gas mixture flows in the experimental cell at a stable pressure and the spectra are acquired summing up several sweeps of the same kinetic energy region. In the latter case, fast switches (in timescale of seconds) between gas mixtures are realized while the evolution of a spectral line is followed in fast-scan mode (time resolution down to the second range[43]). In this study, the Pd $3d_{5/2}$ peak was acquired in snapshot mode, that is, setting the kinetic energy of the analyzer on the centroid of a peak. The kinetic energy window is approximately 1/10 of the selected analyzer pass energy (50 eV in this study), thus 5 eV in this case (+-2.5 eV with respect to the kinetic energy setpoint). A single spectrum of the Pd $3d_{5/2}$ was acquired with a total time resolution of 1.8 sec. Fast gas switches are possible thanks to the flow tube configuration of the cell, where the gas flow can be properly tuned setting the flow rates from mass flow controllers and stabilizing the pressure by means of a diaphragm valve coupled to a root pump downstream. Linearly polarized light was used throughout the experiments.

Palladium foils (99.99% purity, 0.5 mm thickness) were obtained commercially. A 10x10 mm foil was fixed to the manipulator head by means of copper clips. The temperature was monitored with a Pt100 sensor, and the sample was heated by means of a tunable power IR laser (976 nm, maximum power 25 W) projected on the back side of the sample holder. In the

geometry adopted during the experiments, photoelectrons were detected at an angle of 30° with respect to the direction of the surface normal.

The as-introduced foil was heated in oxygen (1 mbar) at 650°C to remove surface carbon contamination, then oxygen was replaced by helium while keeping the temperature stable at 650°C, to fully reduce the sample before starting the experiment. The photoemission spectra of Pd 3d and Pd 3p/O 1s were collected in CH_4+He and then switching to CH_4+O_2 at different temperature steps in the 50-600°C range. The mixture of CH_4+He was also replaced by pure O_2 or CH_4+O_2 +H_2O while measuring XPS. Following this procedure, the oxidation state of palladium at different reaction temperatures and gas mixtures could be followed in situ. An annealing of the sample at 650°C in helium was performed after each reaction step, in order to fully reduce the surface and to always start measuring on the same sample surface. The cleanness and electronic state of palladium was checked by means of XPS (C 1s photoemission signal and wide range scan) after each reaction step, to sort out the accumulation of soot.

The experiments were performed at 1 mbar pressure in different CH_4/O_2 ratios (1:2 and 1:4), in pure oxygen and co-feeding water in the reaction mixture to check its effect on the reactivity (1:4 = CH_4:O_2 molar ratio + 5% H_2O, based on the partial pressures detected in the experimental cell). Ultrapure gases were used throughout the experiments and water vapor was generated from a thermalized reservoir containing Millipore water purified by means of several freeze-pump-thaw cycles. During transient experiments, oxygen was quickly replaced by helium (in the second range) while keeping the pressure in the cell constant at 1 mbar and while acquiring the Pd $3d_{5/2}$ core level peak in snapshot mode.

The Pd 3d and O 1s/Pd 3p spectral regions were recorded using excitation energies of 630 eV and 825 eV, respectively, to collect photoelectrons with approximately the same kinetic

energy of 300 eV, thus generated from the same probed depth. After subtraction of a Shirley background, the photoemission peaks were deconvoluted using Voigt shaped functions. Asymmetric Doniach-Sunjic[48] line shape was used to fit the metallic palladium component of the Pd 3d peaks, in agreement with previous literature reports[49-52]. The position (binding energy scale), full width at half maximum (FWHM) and the line-shapes were constrained during the deconvolution of peak components associated with the same oxidation state. The fitting parameters are listed in Table 1. The error associated to the area of different components obtained from the deconvolution of the Pd 3d signal is the standard deviation calculated repeating the fitting on a statistically relevant sample of spectra collected under the same reaction conditions.

Table 1 Peak fitting parameters (position and FWHM) of Pd 3d and O 1s photoemission spectra

Components		Position (eV)	FWHM (eV)
Pd 3d	Pd(0)	335.95	0.6
	PdO_x	335.6	1.9
	PdO	336.7	0.9
O 1s	O(1)	529.3	1.3
	O(2)	530.2	1.3
	Pd-OH	531.6	1.3

3. Results

Figure 1 shows the Pd 3d spectra measured at 1 mbar in pure oxygen, in a mixture of methane and oxygen in ratios of 1:4 and 1:2, and in a mixture of methane and oxygen in a ratio of 1:4, co-fed with 5% H_2O. The spectra were collected at increasing temperature in the 50°C-600°C range. The red spectra correspond to the reference metal palladium signal, acquired at 50°C immediately after sample cleaning, and are normalized to the maximum intensities and superimposed to the spectra acquired in the low reaction temperature range (150°C-300°C) to highlight the evolution of the peak line shape. In addition, an example of a deconvolution of a Pd $3d_{5/2}$ core level peak is displayed in Figure 1(e). The Pd $3d_{5/2}$ line can be deconvoluted into three components[49-51, 53]: the metal component at 334.95 eV and two oxidic ones shifted towards higher binding energy by 0.65 and 1.7 eV, respectively. Palladium foil exhibits a typical oxidation process from palladium metal (334.95 eV), to a “surface palladium oxide” (335.6 eV), and then to “bulk palladium(II) oxide” (336.7 eV)[53-54]. The two-dimensional surface palladium oxide formed on the surface of Pd (111), was reported to be located at +0.5-+1.3 eV from the metal,[50-51, 53] and its structure was well characterized by LEED and STM[53, 55]. In our experiments, we made use of a polycrystalline foil, thus surface palladium oxide formed on several different crystal facets. Due to the relatively small chamical shifts, all these contributions were convoluted in a single "surface oxide" component, whose full width at half maximum (FWHM) is larger than that of the other components[56]. In this paper, we denote metallic palladium as Pd(0), surface palladium oxide as “surface PdO_x” and bulk palladium(II) oxide as “PdO”. At 50°C, only Pd(0) can be detected. In the absence of water, a shoulder of the main peak, which is assigned to surface PdO_x, appears at 335.6 eV and grows with temperature increasing to 150 and 200°C. At higher temperatures PdO, centered at 336.6 eV, gradually becomes the dominant species. When the temperature reaches 550°C

and 600°C, all palladium oxides are fully reduced to Pd(0). In the presence of water, the formation of surface PdO_x also starts at 150°C, and reaches its maximum value between 150 and 300°C. The peak corresponding to PdO appears only at 350°C, which is 100°C higher than in the water-free methane oxygen mixture at ratio 1:4. Also, in the presence of water, no quantitative reduction of the palladium oxide species happens even at 600 °C.

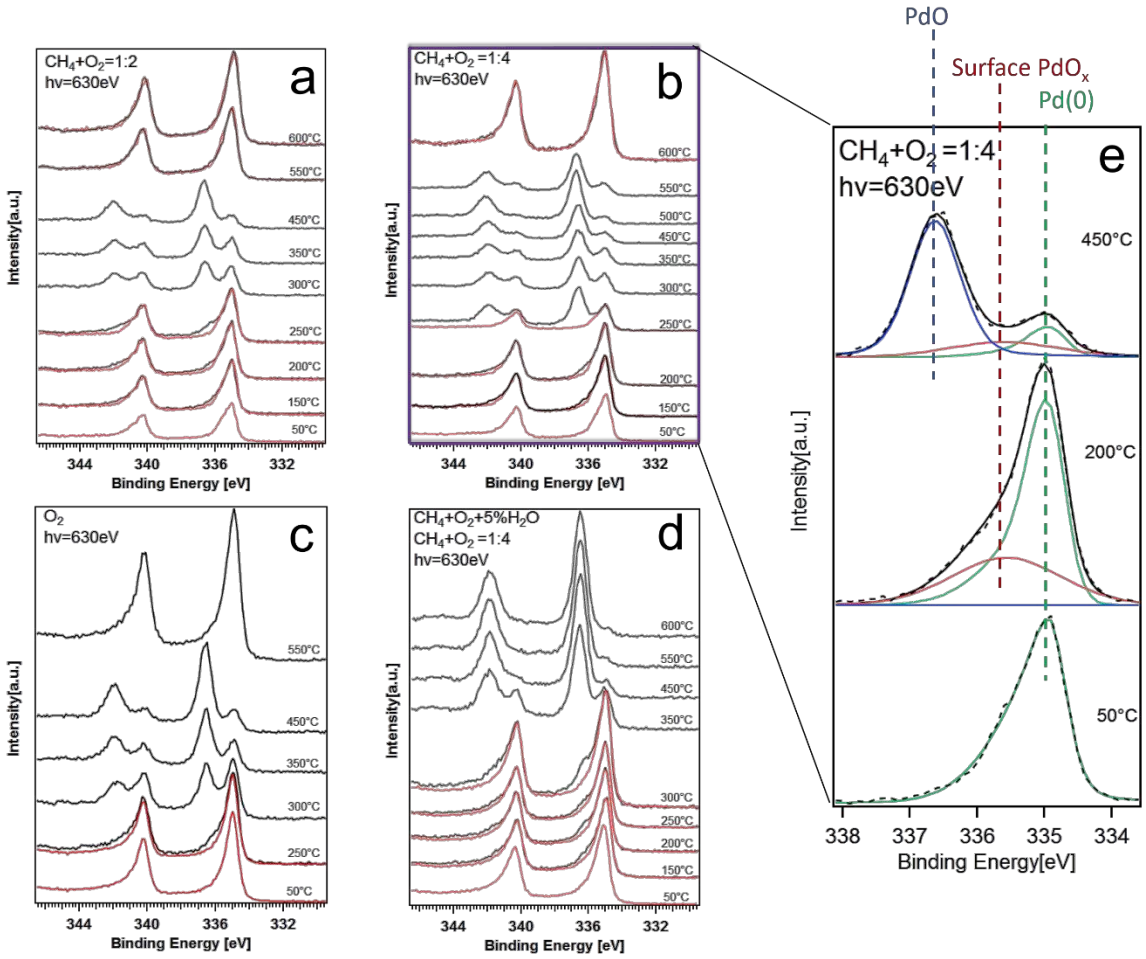

Figure 1 Steady state Pd 3d photoemission spectra in gas atmosphere of (a) CH_4+O_2=1:2, (b)CH_4+O_2=1:4, (c) O_2 only , (d) $CH_4+O_2+5\%H_2O$, CH_4+O_2=1:4 at different temperatures and (e) deconvolution of Pd3d $_{5/2}$ spectra

Figure 2 shows the fraction of each palladium species at different temperatures and in different gas feed environments, evaluated from the deconvolution of the Pd $3d_{5/2}$ spectra of Figure 1. In the first stage, in all the investigated gas compositions, Pd(0) converts into surface

PdO_x. With increasing temperature (>300°C), the percentages of both surface PdO_x and Pd(0) decrease, whereas that of PdO increases and becomes the highest. The onset of surface PdO_x growth is similar in all the investigated reaction environments, starting at 100°C, whereas the evolution of PdO shows variation depending on the gas environment. A 50°C delay compared to the reaction mixture (methane + oxygen) is observed when only oxygen is dosed. Such a delay could be caused by the formation of an oxide skin in the presence of only oxygen, which could protect the metal from being further oxidized[57]. When methane is co-dosed in the reaction mixture, it reacts with the protection layer, and the formation of bulk oxide starts at lower temperature. The shift increases to 100°C when water is co-fed. The decreased oxidation to bulk PdO in the presence of water suggests either the hindrance of oxygen activation and of its diffusion[26]. Interestingly, the interval of stability of surface PdO_x with the temperature is larger (from 100 to 300°C) when water is co-dosed. For different CH_4/O_2 ratios,there is a subtle change in the onset of growth of PdO. This could be due either to a morphological change of the foil in the presence of methane, or to a different amount of water generated at different CH_4/O_2 ratios. At 600°C, the highest investigated reaction temperature, all the palladium oxide species are reduced back to Pd(0), except in the case when water is co-dosed in the reaction mixture.

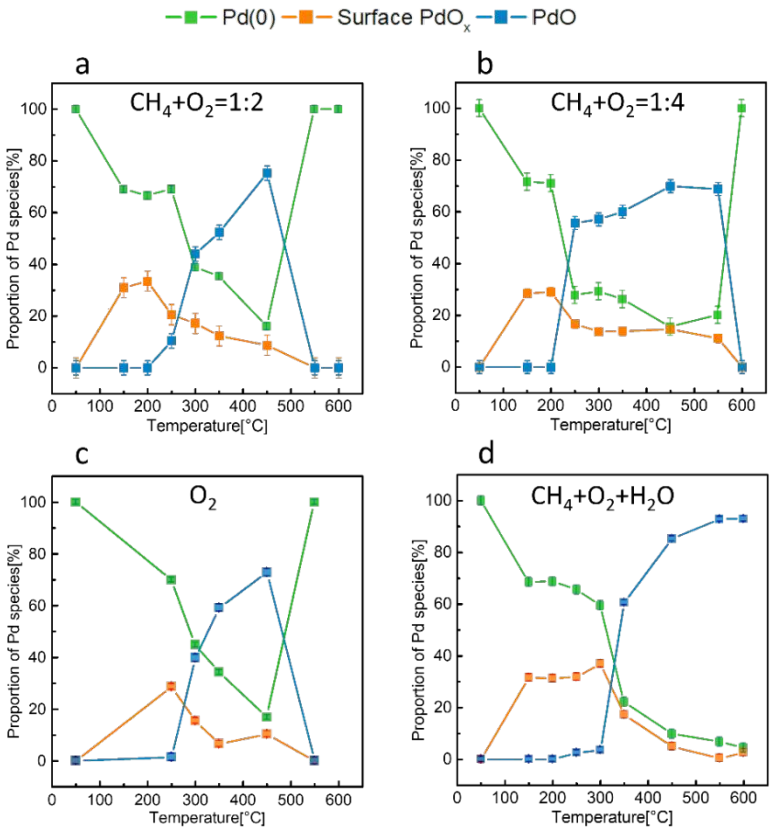

Figure 2 Proportion of Pd(0), surface PdO_x and PdO in gas atmosphere of (a) CH_4+O_2=1:2, (b)CH_4+O_2=1:4, (c) O_2 only , (d) CH_4+O_2+5%H_2O, CH_4+O_2=1:4 at different temperatures

Surface hydroxyls are expected to form on the surface of palladium foil both during the reaction (hydrogen abstraction from adsorbed methyl groups) and when water is co-dosed[14, 58]. However, the peak of surface palladium hydroxyls (Pd-OH) is reported to overlap with the surface PdO_x in the Pd 3d photoemission spectra[59]. To elucidate the effect of water dosing during the methane oxidation reaction, and to monitor the amount surface hydroxyls, we also acquired the Pd $3p_{3/2}$/O 1s photoemission spectral region exposing the sample to a 1:4 methane + oxygen reaction mixture with and without co-dosing water (Figure 3 (a)). A temperature of 450°C was selected because in both cases the amount of PdO reaches its maximum. Figure 3(b) displays the deconvolution of the Pd $3p_{3/2}$ and of the O 1s

photoemission peaks, which appear in a similar binding energy range. In the Pd $3p_{3/2}$ region, we fixed the surface PdO_x / PdO ratio to 0.21 and 0.058 for water-free and water-dosed samples, respectively, which is consistent with the ratios extrapolated from the deconvolution of the Pd 3d. As reported in reference [55], the O 1s peaks centered at 528.8 and 529.6 eV are assigned to surface palladium oxide. Therefore, in our experiment the low-BE peak, i.e. O(1), at 529.3 eV, corresponds to the topmost layer oxygen of surface PdO_x whereas O(2) at 530.2 eV is assigned to bulk PdO[55-56]. The third component, centered at 531.6 eV, can be clearly observed in both reaction environments and particularly in the presence of water. The peak can be assigned to palladium-coordinated hydroxyl groups (Pd-OH)[59-60], which form both during the methane oxidation reaction and by reaction with water (when dosed in the feed). We calculate and list the oxygen species proportion under water/water-free conditions in Table 2. The concentration of O(1) reduces by 6%, passing from 11% to 5%, while the fraction of surface hydroxyls increases by 3.5 times, passing from 4% to 14%. The fraction of O(2) is relatively constant.

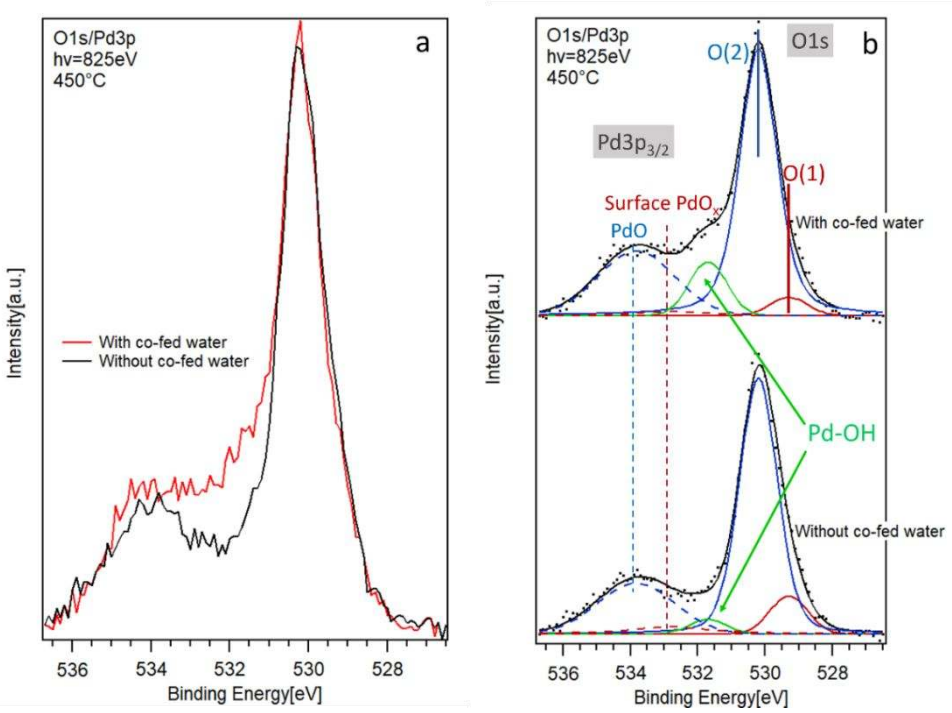

Figure 3 (a)Photoemission spectra of O 1s and Pd $3p_{3/2}$ in the reaction gas of CH_4+O_2 and CH_4+O_2+5%H_2O and (b) deconvolution of the spectra at 450°C.

Table 2 Proportion of oxygen species in the reaction gas of CH_4+O_2 and CH_4+O_2+5%H_2O at 450°C. Calculated from O 1s deconvolution results.

O 1s species	Oxygen species proportion (%) without water	Oxygen species proportion (%) with water
O(1)	11.3±0.6	4.7±0.6
O(2)	84.4±0.6	81.5±1.8
-OH	4.3±0.4	13.8±1.7

We also compared the evolution of palladium species by means of time-resolved experiments performed under transient conditions, to characterize the formation process of the palladium oxides. The reaction environment was modified switching from a mixture not containing the oxidant (CH_4+He) to one containing it (CH_4+O_2 respectively CH_4+O_2+H_2O) while acquiring snapshots of the Pd $3d_{5/2}$ spectrum (as reported in the experimental methods section). As an example, Figure 4 shows a series of snapshots of the Pd $3d_{5/2}$ signal collected while switching from CH_4+He to CH_4+O_2 (1:4) at 450°C. The color scale in figure 4(a) indicates the peaks location (bright regions) and their development as a function of time (1 iteration corresponds to 1 snapshot of the Pd $3d_{5/2}$, thus to 1.8 seconds). Because no clear modifications of the Pd $3d_{5/2}$ were evident comparing single snapshots, we summed up 20 consecutive iterations (corresponding to a time resolution of 36 seconds). As expected, the palladium foil was quickly oxidized after replacing helium with oxygen, and the evolution of the line shape of the spectra is shown in Figure 4(b).

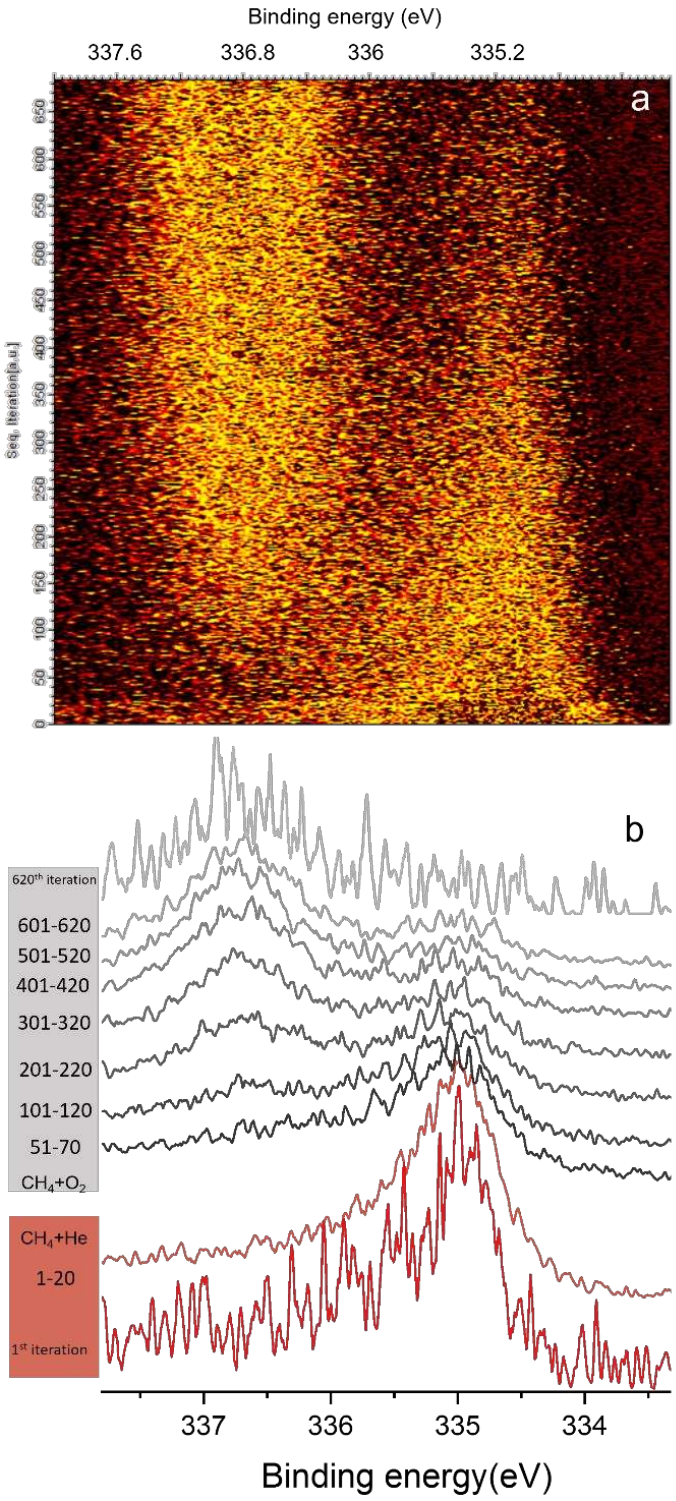

Figure 4 Evolution of (a) Pd $3d_{5/2}$ spectra and (b) dimension-reduced Pd $3d_{5/2}$ spectra after switching from CH_4+He to CH_4+O_2 at 450°C. The plot shows (for comparison) single snapshots (1st and 620th iteration) and the sum of 20 iterations (used for the deconvolution process and for the analysis of the time-evolution of the palladium species) collected under both reaction conditions.

The summed spectra were deconvoluted using the parameters obtained from the analysis of the high resolution spectra (Table 1 and Figure 1(e)) and the percentage of each single component is plotted as a function of time in Figure 5. All the plots show a common behavior: after a transient period, whose duration depends on the reaction environment and on the temperature and during which the percentage of the components varies sensibly, a plateau is reached, which corresponds to the steady-state conditions. The decrease of Pd(0) and the increase of surface PdO_x and of PdO indicates the gradual oxidation of the palladium foil when it is exposed to the methane oxidation reaction mixture. The initial formation rate of surface PdO_x is always higher or at least equal to that of PdO, which implies that surface PdO_x is the precursor of lattice PdO. More importantly, the initial formation of surface PdO_x and that of PdO display a slow-fast-slow process with temperature, visible in both reaction mixtures (Figure 5a and 5b and Table 2). The fastest initial formation rate of PdO and of surface PdO_x detected while dosing a CH_4+O_2 (1:4) mixture is found at 350°C. In the presence of water, the fastest initial formation rate of PdO and of surface PdO_x shifts to 450°C. Therefore, the addition of water to a methane combustion reaction mixture causes a positive shifts of the temperature at which the fastest oxidation of palladium takes place. Such a temperature shift correlates well with the analysis of the palladium species as a function of the reaction temperature discussed above (Figure 2). The evolution of the palladium species at 600°C in Figure 5 is also in agreement with the steady state results of Figure 2, i.e. no PdO formation is observed in the absence of water, whereas a gradual oxidation still takes place when water is co-dosed.

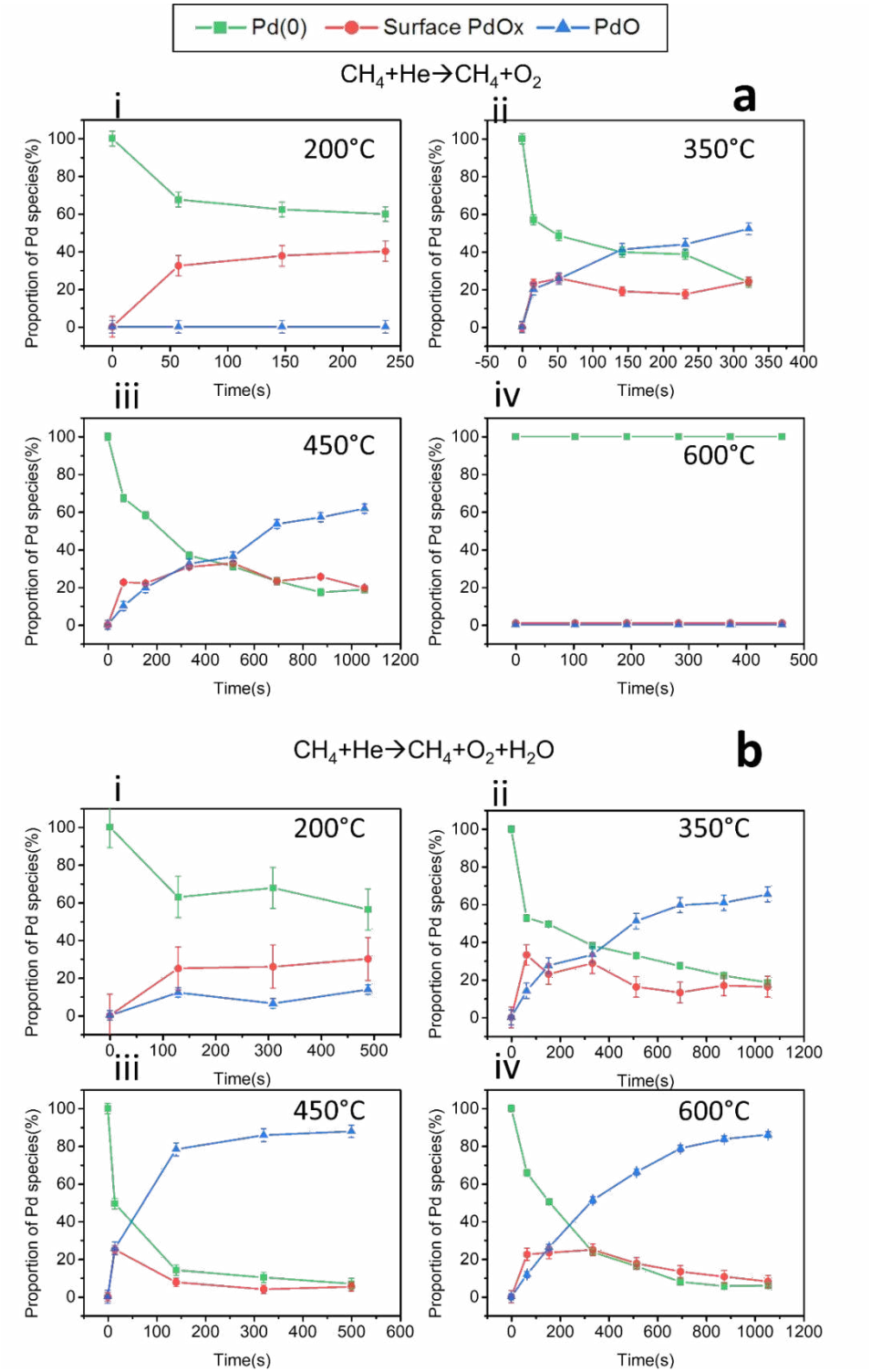

Figure 5 Time-resolved evolution of palladium species after switching from (a) CH_4+He to CH_4+O_2 and (b) CH_4+He to CH_4+O_2+5%H_2O

4. Discussion

Our main goal was to determine the influence of water on the structure of palladium catalyst for methane combustion. The interactions between the reagents and the catalyst surface in the absence and in the presence of water are important to follow the reaction mechanism and to identify the active sites involved.

It is commonly accepted that the addition of water causes a decrease of the catalytic activity of palladium catalysts. Kinetics results about methane combustion reaction over palladium model catalyst[2, 23] and nano-scale catalyst[14] reported similar reaction order for water, ranging from -0.9 to -1.1. This means that water has inhibition effect on both Pd foil and on supported Pd catalysts. To explain such an effect, it has been postulated that water blocks palladium active sites, forming either palladium hydroxide[8, 58] or surface hydroxyls[14, 26].

The formation of hydroxyl groups detected in Figure 3 supports the assumption that the palladium active sites are blocked by hydroxyls. Surface palladium hydroxyl groups form both in the absence and in the presence of water. The peak of $Pd(OH)_2$ was not detected at 337.4 eV[61] when water was co-fed, which indicates that bulk palladium hydroxide is not the cause of water inhibition effect over palladium foil. Notably, the percentage of hydroxyls increases considerably when water is co-dosed with the reaction mixture, mostly at the expense of surface PdO_x. The presence of water in the feed converts dominantly the surface PdO_x into palladium hydroxyls, as shown in Figure 3 and Table 2. This also indicates that the active sites for methane activation are on surface PdO_x. More specifically, coordinatively unsaturated palladium (hereafter called Pd_{cus}) sites are contained in the polycrystalline surface PdO_x spectral component, and their role in the mechanism of methane combustion is confirmed in several literature reports[14, 58, 62-63].

As already mentioned in the introduction, Fujimoto et al.[14] proposed a sequence of reaction pathways in which the catalytic sites are coordinatively unsaturated palladium atoms and oxygen vacancies on the surface of PdO crystallites. Gaseous methane first binds to the Pd_{cus} sites, then hydrogen atoms are gradually abstracted by the adjacent surface Pd-O sites and yield Pd-OH. Water is generated by the quasi-equilibrated condensation of surface hydroxyls and its desorption generates oxygen vacancies (hereafter called O_v). In this case, water favors the reverse reaction of hydroxyl recombination (i.e. palladium hydroxyl generation), described as:

$$H_2O + Pd\text{-}O + Pd\text{-}O_v \rightleftharpoons 2\ Pd\text{-}OH \qquad (2)$$

Stotz et al.[58] proposed another reaction route envisaging H-abstraction from $Pd\text{-}CH_2O$ that generates water. This step also generates carbon intermediates and releases Pd_{cus} sites, and can be described as:

$$Pd\text{-}CHOH + Pd\text{-}OH \rightleftharpoons H_2O + Pd\text{-}CHO + Pd_{cus} \qquad (3)$$

Based on the literature reports shown above, methane adsorption requires coordinatively unsaturated palladium sites (Pd_{cus}), while adjacent oxidic sites (Pd-O) are necessary to abstract the hydrogen forming hydroxyl groups. Notably, the inhibition of Pd_{cus} sites indicates that water competes with methane for the same adsorption sites. Water adsorbs on the Pd_{cus} sites and is then deprotonated by adjacent surface Pd-O sites forming surface hydroxyls. As a consequence of this, the H-abstraction process of methyl intermediates does not take place. The reaction (2) and reverse reaction (3) explain the negative order in water[14] in the rate equation (1), which we experimentally correlate with the formation of surface palladium hydroxyls. Our study shows that the fraction of surface PdO_x reaches its maximum in a limited

temperature range, which is between 100 and 200°C for the 1:2 and 1:4 CH_4:O_2 reaction mixtures and extends to 300°C both in pure oxygen and when water is co-dosed. A decrease of the fraction of surface PdO_x corresponds to the increase of the PdO population. Therefore, surface PdO_x acts as a precursor of the bulk PdO, as also confirmed by the correlation of the time-evolution of the surface PdO_x component with that of PdO (Figure 5 and Table 2). Interestingly, the intensity of the surface PdO_x component evaluated from the Pd $3d_{5/2}$ is not reaching zero in the temperature range where PdO is stable (Figure 2). This is due to two reasons:

i) Patches of surface PdO_x are stable at high temperatures, as shown when pure oxygen is dosed on palladium foil, thus no source of hydrogen is present [64](see Figure 2(c)).

ii) Hydroxyl groups are formed during the methane oxidation reaction. The photoemission peak associated with surface Pd-OH and the one of surface PdO_x are superimposed in the Pd 3d spectral region[60]. Therefore, the 335.6 eV signal detected at T>200°C is also due to Pd-OH formed during hydrogen abstraction form methane, as clearly seen in Figure 1b and Figure 3b, without dosing water.

Because in our deconvolution of the Pd 3d we made use of a single peak to fit the surface PdO_x, we would like to stress that such a component contains three different kind of palladium surface oxide sites, and namely 2-coordinated palladium, 4-coordinated palladium and palladium hydroxyl[56, 60, 65].Therefore, water inhibition could affect Pd_{cus} as well as surface oxygen vacancies. For instance, the adsorption of water was recently observed on Pd/ZrO_2 catalyst[66]. Transformation of t-ZrO_2 to m-ZrO_2 forms oxygen vacancies and water weakens the

promotion effect by the blocking of vacancy sites. The migration of oxygen vacancies is important in the reduction and oxidation process of palladium[67].

As shown in Figure 2 and listed in Table 3, during our in situ steady state and transient measurements, we observed the concurrent postponement in PdO formation and a shift of the maximum palladium oxide initial formation rate in the presence of water, respectively. The temperature delay is 100°C, which correlates well with the methane combustion reactivity tests on palladium catalysts[24, 60]. Typically, when water is added to the reaction mixture, a positive shift (35-120°C temperature range) of T_{50} (temperature at which 50% methane conversion is achieved) is measured[25, 68]. The turnover rate for methane oxidation was found to decrease by 95% when PdO decomposed to Pd metal at 888 K, showing that PdO is more active than Pd metal for methane combustion at this temperature[69]. The Pd-O site is always considered as the activation site of methane, however, no agreement has been reached on whether PdO is the site of oxygen activation. In the traditional Mars-van-Krevelen redox mechanism for methane oxidation, the oxygen vacancies are always healed by gaseous oxygen[14, 58]. Other reports claimed that the vacancy is filled by bulk PdO when the oxygen partial pressure above the catalyst is low, otherwise the oxygen vacancy will adsorb oxygen from the gas phase[70]. Experiments carried out making use of isotopically labeled reaction mixtures gave more details about the oxygen distribution in the reaction products, i.e. in water. At 600 K, the oxygen in H_2O is entirely coming from the PdO lattice. Burch[21] also reported that oxygen chemisorbed on palladium metal is poorly active and that the methane conversion curve increases simultaneously to reach a plateau at the point where Pd has taken up about the equivalent of 3 monolayers of oxygen. Importantly, no further increase (or decrease) in the activity of the catalyst was observed after bulk PdO was formed. Martin et

al. found that the efficiency of the methane oxidation reaction was strongly promoted by the presence of an oxygen atom directly underneath the Pd_{cus} atom in the PdO(101) structure with a ligand effect. The role of the oxygen atom is to induce a reduction of the Pauli repulsion between the Pd_{cus} and the CH_4 molecule, which facilitates the C-H bond activation. Therefore, bulk PdO can be considered an important active phase for the methane oxidation, because of providing oxygen and/or ligand effect. Based on these results, we can correlate the postponement in the formation of PdO observed in this study in the presence of water to the shift of the methane conversion curve observed experimentally on methane oxidation catalysts.

Table 3. Initial formation rate of PdO and surface PdO_x with water on/off at different temperatures

Temperature/°C	Initial formation rate of PdO[a.u.]		Initial formation rate of surface PdO_x[a.u.]	
	With water	Without water	With water	Without water
200	0.00094	0	0.0019	0.0056
350	0.0016	0.0070	0.0037	0.014
450	0.018	0.0016	0.018	0.0035
600	0.0013	0	0.0025	0

Such a shift is due to the inhibition of oxygen vacancies by water. As the XPS results show and as reported in references [65, 67, 71], the surface PdO_x is the precursor of PdO. The bulk-surface oxygen exchange requires the migration of oxygen vacancies. This step is described as:

$$\text{Pd-O(surface)} + \text{Pd(bulk)} \rightleftharpoons \text{PdO(bulk)} + \text{Pd-O}_v \quad (4)$$

In the oxidation process, the vacancies are healed by gaseous oxygen. When water is co-dosed with the reagents, surface hydroxyls form and block the oxygen vacancies, thus the migration of oxygen. Consequently, PdO formation is delayed. Finally, upon recombination of Pd-OH and water desorption, oxygen from the gas phase can react efficiently with the surface and

the formation of a thicker PdO layer starts by the migration of oxygen between bulk and surface. Because PdO contributes to the methane oxidation reaction healing the oxygen vacancies left after Pd-OH recombination, this effect may contribute to the water-mediated inhibition of the catalyst.

5. Conclusions

Ambient pressure X-ray photoelectron spectroscopy was used to investigate in situ the palladium electronic states in the complete oxidation of methane on a palladium foil, and the effect of water co-dosing. The evolution of Pd(0), of surface PdO_x and of PdO were followed at different temperatures and under different gas environments. The main conclusions are:

1. Water inhibits the methane combustion reaction by converting surface palladium oxide to surface hydroxyls. Palladium hydroxyls block the coordinatively unsaturated palladium sites for methane adsorption and adjacent oxidic sites for methane activation. The hydrogen-abstraction process of methyl reaction intermediates is also inhibited. Palladium hydroxide formation is not the consequence of water inhibition effect over palladium catalysts for the combustion of methane on palladium foil.

2. Water adsorbs on surface oxygen vacancies, followed by its deprotonation and the formation of a second hydroxyl on a neighboring Pd-O site. The formation of a relevant amount of surface palladium hydroxyls in the presence of water hinders the adsorption of oxygen from the gas phase, postponing the formation of bulk PdO. Consequently, in the presence of water, the oxygen vacancy sites cannot be filled by oxygen migration from the bulk, and this effect contributes to the water inhibition effect on the combustion of methane.

Author information

Corresponding authors

*E-mail: luca.artiglia@psi.ch.

*E-mail: jeroen.vanbokhoven@chem.ethz.ch

Notes

The authors declare no competing financial interest.

Acknowledgments

X.L. and X.W. acknowledge financial support from the China Scholarship Council.

References

1. Chu, S.; Majumdar, A., Opportunities and challenges for a sustainable energy future. *Nature* **2012,** *488*, 294.
2. Zhu, G.; Han, J.; Zemlyanov, D. Y.; Ribeiro, F. H., The Turnover Rate for the Catalytic Combustion of Methane over Palladium Is Not Sensitive to the Structure of the Catalyst. *J. Am. Chem. Soc.* **2004,** *126* (32), 9896-9897.
3. Lv, C.-Q.; Ling, K.-C.; Wang, G.-C., Methane combustion on Pd-based model catalysts: Structure sensitive or insensitive? *The Journal of chemical physics* **2009,** *131* (14), 144704.
4. Stettler, M. E. J.; Midgley, W. J. B.; Swanson, J. J.; Cebon, D.; Boies, A. M., Greenhouse Gas and Noxious Emissions from Dual Fuel Diesel and Natural Gas Heavy Goods Vehicles. *Environmental Science & Technology* **2016,** *50* (4), 2018-2026.
5. Liu, Z.-P.; Hu, P., General Rules for Predicting Where a Catalytic Reaction Should Occur on Metal Surfaces: A Density Functional Theory Study of C−H and C−O Bond Breaking/Making on Flat, Stepped, and Kinked Metal Surfaces. *J. Am. Chem. Soc.* **2003,** *125* (7), 1958-1967.
6. Gélin, P.; Primet, M., Complete oxidation of methane at low temperature over noble metal based catalysts: a review. *Applied Catalysis B: Environmental* **2002,** *39* (1), 1-37.
7. Farrauto, R. J.; Hobson, M.; Kennelly, T.; Waterman, E., Catalytic chemistry of supported palladium for combustion of methane. *Applied Catalysis A: General* **1992,** *81* (2), 227-237.
8. Burch, R.; Urbano, F. J.; Loader, P. K., Methane combustion over palladium catalysts: The effect of carbon dioxide and water on activity. *Applied Catalysis A: General* **1995,** *123* (1), 173-184.
9. Zhu, G.; Han, J.; Zemlyanov, D. Y.; Ribeiro, F. H., Temperature dependence of the kinetics for the complete oxidation of methane on palladium and palladium oxide. *The Journal of Physical Chemistry B* **2005,** *109* (6), 2331-2337.
10. Persson, K.; Pfefferle, L. D.; Schwartz, W.; Ersson, A.; Järås, S. G., Stability of palladium-based catalysts during catalytic combustion of methane: The influence of water. *Applied Catalysis B: Environmental* **2007,** *74* (3), 242-250.
11. Cargnello, M.; Jaén, J. J. D.; Garrido, J. C. H.; Bakhmutsky, K.; Montini, T.; Gámez, J. J. C.; Gorte, R. J.; Fornasiero, P., Exceptional Activity for Methane Combustion over Modular Pd@CeO_2 units on Functionalized Al_2O_3. *Science* **2012,** *337* (6095), 713-717.
12. Cullis, C. F.; Nevell, T. G.; Trimm, D. L., Role of the catalyst support in the oxidation of methane over palladium. *Journal of the Chemical Society, Faraday Transactions 1: Physical Chemistry in Condensed Phases* **1972,** *68* (0), 1406-1412.
13. Ribeiro, F. H.; Chow, M.; Dallabetta, R. A., Kinetics of the Complete Oxidation of Methane over Supported Palladium Catalysts. *Journal of Catalysis* **1994,** *146* (2), 537-544.
14. Fujimoto, K.-i.; Ribeiro, F. H.; Avalos-Borja, M.; Iglesia, E., Structure and Reactivity of PdO_x/ZrO_2 Catalysts for Methane Oxidation at Low Temperatures. *Journal of Catalysis* **1998,** *179* (2), 431-442.
15. Hoflund, G. B.; Hagelin, H. A. E.; Weaver, J. F.; Salaita, G. N., ELS and XPS study of Pd/PdO methane oxidation catalysts. *Applied Surface Science* **2003,** *205* (1), 102-112.
16. Han, J.; Zemlyanov, D. Y.; Ribeiro, F. H., Catalytic combustion of methane on palladium single crystals. *Catalysis Today* **2006,** *117* (4), 506-513.
17. Meng, L.; Lin, J.-J.; Pu, Z.-Y.; Luo, L.-F.; Jia, A.-P.; Huang, W.-X.; Luo, M.-F.; Lu, J.-Q., Identification of active sites for CO and CH_4 oxidation over PdO/$Ce_{1-x}Pd_xO_{2-\delta}$ catalysts. *Applied Catalysis B: Environmental* **2012,** *119-120*, 117-122.
18. Bossche, M. V. d.; Grönbeck, H., Methane Oxidation over PdO(101) Revealed by First-Principles Kinetic Modeling. *J. Am. Chem. Soc.* **2015,** *137* (37), 12035-12044.
19. Colussi, S.; Gayen, A.; Farnesi Camellone, M.; Boaro, M.; Llorca, J.; Fabris, S.; Trovarelli, A., Nanofaceted Pd-O Sites in Pd-Ce Surface Superstructures: Enhanced Activity in Catalytic Combustion of Methane. *Angewandte Chemie International Edition* **2009,** *48* (45), 8481-8484.

20. Willis, J. J.; Gallo, A.; Sokaras, D.; Aljama, H.; Nowak, S. H.; Goodman, E. D.; Wu, L.; Tassone, C. J.; Jaramillo, T. F.; Abild-Pedersen, F.; Cargnello, M., Systematic Structure–Property Relationship Studies in Palladium-Catalyzed Methane Complete Combustion. *ACS Catal.* **2017,** *7* (11), 7810-7821.
21. Burch, R., Low NO_x options in catalytic combustion and emission control. *Catalysis Today* **1997,** *35* (1), 27-36.
22. Duan, H.; You, R.; Xu, S.; Li, Z.; Qian, K.; Cao, T.; Huang, W.; Bao, X., Pentacoordinated Al^{3+}-Stabilized Active Pd Structures on Al_2O_3-Coated Palladium Catalysts for Methane Combustion. *Angewandte Chemie International Edition* **2019,** *58* (35), 12043-12048.
23. Monteiro, R. S.; Zemlyanov, D.; Storey, J. M.; Ribeiro, F. H., Turnover Rate and Reaction Orders for the Complete Oxidation of Methane on a Palladium Foil in Excess Dioxygen. *Journal of Catalysis* **2001,** *199* (2), 291-301.
24. Zhang, F.; Hakanoglu, C.; Hinojosa, J. A.; Weaver, J. F., Inhibition of methane adsorption on PdO(101) by water and molecular oxygen. *Surface Science* **2013,** *617*, 249-255.
25. Petrov, A. W.; Ferri, D.; Krumeich, F.; Nachtegaal, M.; van Bokhoven, J. A.; Kröcher, O., Stable complete methane oxidation over palladium based zeolite catalysts. *Nature Communications* **2018,** *9* (1), 2545.
26. Schwartz, W. R.; Ciuparu, D.; Pfefferle, L. D., Combustion of Methane over Palladium-Based Catalysts: Catalytic Deactivation and Role of the Support. *The Journal of Physical Chemistry C* **2012,** *116* (15), 8587-8593.
27. Barrett, W.; Shen, J.; Hu, Y.; Hayes, R. E.; Scott, R. W. J.; Semagina, N., Understanding the Role of SnO_2 Support in Water-Wolerant Methane Combustion: In situ Observation of $Pd(OH)_2$ and Comparison with Pd/Al_2O_3. *ChemCatChem* **2020,** *12* (3), 944-952.
28. Toso, A.; Colussi, S.; Llorca, J.; Trovarelli, A., The dynamics of PdO-Pd phase transformation in the presence of water over Si-doped Pd/CeO_2 methane oxidation catalysts. *Applied Catalysis A: General* **2019,** *574*, 79-86.
29. Gholami, R.; Smith, K. J., Activity of PdO/SiO_2 catalysts for CH_4 oxidation following thermal treatments. *Applied Catalysis B: Environmental* **2015,** *168-169*, 156-163.
30. Lustemberg, P. G.; Palomino, R. M.; Gutiérrez, R. A.; Grinter, D. C.; Vorokhta, M.; Liu, Z.; Ramírez, P. J.; Matolín, V.; Ganduglia-Pirovano, M. V.; Senanayake, S. D.; Rodriguez, J. A., Direct Conversion of Methane to Methanol on Ni-Ceria Surfaces: Metal–Support Interactions and Water-Enabled Catalytic Conversion by Site Blocking. *J. Am. Chem. Soc.* **2018,** *140* (24), 7681-7687.
31. Velin, P.; Ek, M.; Skoglundh, M.; Schaefer, A.; Raj, A.; Thompsett, D.; Smedler, G.; Carlsson, P.-A., Water Inhibition in Methane Oxidation over Alumina Supported Palladium Catalysts. *The Journal of Physical Chemistry C* **2019,** *123* (42), 25724-25737.
32. Huang, W.; Goodman, E. D.; Losch, P.; Cargnello, M., Deconvoluting Transient Water Effects on the Activity of Pd Methane Combustion Catalysts. *Industrial & Engineering Chemistry Research* **2018,** *57* (31), 10261-10268.
33. Gremminger, A. T.; Pereira de Carvalho, H. W.; Popescu, R.; Grunwaldt, J.-D.; Deutschmann, O., Influence of gas composition on activity and durability of bimetallic $Pd\text{-}Pt/Al_2O_3$ catalysts for total oxidation of methane. *Catalysis Today* **2015,** *258*, 470-480.
34. Nassiri, H.; Lee, K.-E.; Hu, Y.; Hayes, R. E.; Scott, R. W. J.; Semagina, N., Water shifts PdO-catalyzed lean methane combustion to Pt-catalyzed rich combustion in Pd–Pt catalysts: In situ X-ray absorption spectroscopy. *Journal of Catalysis* **2017,** *352*, 649-656.
35. Ersson, A.; Kušar, H.; Carroni, R.; Griffin, T.; Järås, S., Catalytic combustion of methane over bimetallic catalysts a comparison between a novel annular reactor and a high-pressure reactor. *Catalysis Today* **2003,** *83* (1), 265-277.
36. Alyani, M.; Smith, K. J., Kinetic Analysis of the Inhibition of CH_4 Oxidation by H_2O on PdO/Al_2O_3 and $CeO_2/PdO/Al_2O_3$ Catalysts. *Industrial & Engineering Chemistry Research* **2016,** *55* (30), 8309-8318.
37. Monteiro, R. S.; Zemlyanov, D.; Storey, J. M.; Ribeiro, F. H., Surface Area Increase on Pd Foils after Oxidation in Excess Methane. *Journal of Catalysis* **2001,** *201* (1), 37-45.

38. Weckhuysen, B. M., Snapshots of a working catalyst: possibilities and limitations of in situ spectroscopy in the field of heterogeneous catalysis. *Chemical Communications* **2002,** (2), 97-110.
39. Rodríguez, J. A.; Hanson, J. C.; Chupas, P. J., *In-situ characterization of heterogeneous catalysts*. Wiley Online Library: 2013; Vol. 1.
40. Li, X.; Yang, X.; Zhang, J.; Huang, Y.; Liu, B., In Situ/Operando Techniques for Characterization of Single-Atom Catalysts. *ACS Catal.* **2019,** *9* (3), 2521-2531.
41. Karslıoğlu, O.; Bluhm, H., Ambient-Pressure X-ray Photoelectron Spectroscopy (APXPS). In *Operando Research in Heterogeneous Catalysis*, Frenken, J.; Groot, I., Eds. Springer International Publishing: Cham, 2017; pp 31-57.
42. Roy, K.; Artiglia, L.; van Bokhoven, J. A., Ambient Pressure Photoelectron Spectroscopy: Opportunities in Catalysis from Solids to Liquids and Introducing Time Resolution. *ChemCatChem* **2018,** *10* (4), 666-682.
43. Artiglia, L.; Orlando, F.; Roy, K.; Kopelent, R.; Safonova, O.; Nachtegaal, M.; Huthwelker, T.; van Bokhoven, J. A., Introducing Time Resolution to Detect Ce^{3+} Catalytically Active Sites at the Pt/CeO_2 Interface through Ambient Pressure X-ray Photoelectron Spectroscopy. *The Journal of Physical Chemistry Letters* **2017,** *8* (1), 102-108.
44. Artiglia, L.; Sushkevich, V. L.; Palagin, D.; Knorpp, A. J.; Roy, K.; van Bokhoven, J. A., In Situ X-ray Photoelectron Spectroscopy Detects Multiple Active Sites Involved in the Selective Anaerobic Oxidation of Methane in Copper-Exchanged Zeolites. *ACS Catal.* **2019,** *9* (8), 6728-6737.
45. Ammann, M.; Artiglia, L.; Bartels-Rausch, T., Chapter 6 - X-Ray Excited Electron Spectroscopy to Study Gas–Liquid Interfaces of Atmospheric Relevance. In *Physical Chemistry of Gas-Liquid Interfaces*, Faust, J. A.; House, J. E., Eds. Elsevier: 2018; pp 135-166.
46. Artiglia, L.; Edebeli, J.; Orlando, F.; Chen, S.; Lee, M.-T.; Corral Arroyo, P.; Gilgen, A.; Bartels-Rausch, T.; Kleibert, A.; Vazdar, M.; Andres Carignano, M.; Francisco, J. S.; Shepson, P. B.; Gladich, I.; Ammann, M., A surface-stabilized ozonide triggers bromide oxidation at the aqueous solution-vapour interface. *Nature Communications* **2017,** *8* (1), 700.
47. Orlando, F.; Waldner, A.; Bartels-Rausch, T.; Birrer, M.; Kato, S.; Lee, M.-T.; Proff, C.; Huthwelker, T.; Kleibert, A.; van Bokhoven, J.; Ammann, M., The Environmental Photochemistry of Oxide Surfaces and the Nature of Frozen Salt Solutions: A New in Situ XPS Approach. *Topics in Catalysis* **2016,** *59* (5), 591-604.
48. Doniach, S.; Sunjic, M., Many-electron singularity in X-ray photoemission and X-ray line spectra from metals. *Journal of Physics C: Solid State Physics* **1970,** *3* (2), 285.
49. Teschner, D.; Pestryakov, A.; Kleimenov, E.; Hävecker, M.; Bluhm, H.; Sauer, H.; Knop-Gericke, A.; Schlögl, R., High-pressure X-ray photoelectron spectroscopy of palladium model hydrogenation catalysts.: Part 1: Effect of gas ambient and temperature. *Journal of Catalysis* **2005,** *230* (1), 186-194.
50. Zemlyanov, D.; Aszalos-Kiss, B.; Kleimenov, E.; Teschner, D.; Zafeiratos, S.; Hävecker, M.; Knop-Gericke, A.; Schlögl, R.; Gabasch, H.; Unterberger, W., In situ XPS study of Pd (111) oxidation. Part 1: 2D oxide formation in 10^{-3} mbar O_2. *Surface science* **2006,** *600* (5), 983-994.
51. Ketteler, G.; Ogletree, D. F.; Bluhm, H.; Liu, H.; Hebenstreit, E. L. D.; Salmeron, M., In Situ Spectroscopic Study of the Oxidation and Reduction of Pd(111). *J. Am. Chem. Soc.* **2005,** *127* (51), 18269-18273.
52. Toyoshima, R.; Yoshida, M.; Monya, Y.; Kousa, Y.; Suzuki, K.; Abe, H.; Mun, B. S.; Mase, K.; Amemiya, K.; Kondoh, H., In Situ Ambient Pressure XPS Study of CO Oxidation Reaction on Pd(111) Surfaces. *The Journal of Physical Chemistry C* **2012,** *116* (35), 18691-18697.
53. Lundgren, E.; Kresse, G.; Klein, C.; Borg, M.; Andersen, J. N.; De Santis, M.; Gauthier, Y.; Konvicka, C.; Schmid, M.; Varga, P., Two-Dimensional Oxide on Pd(111). *Physical Review Letters* **2002,** *88* (24), 246103.
54. Todorova, M.; Lundgren, E.; Blum, V.; Mikkelsen, A.; Gray, S.; Gustafson, J.; Borg, M.; Rogal, J.; Reuter, K.; Andersen, J. N.; Scheffler, M., The Pd(100) $-(\sqrt{5}\times\sqrt{5})R27^\circ$ -O surface oxide revisited. *Surface Science* **2003,** *541* (1), 101-112.

55. Titkov, A. I.; Salanov, A. N.; Koscheev, S. V.; Boronin, A. I., Mechanisms of Pd(110) surface reconstruction and oxidation: XPS, LEED and TDS study. *Surface Science* **2006,** *600* (18), 4119-4125.
56. Kibis, L. S.; Titkov, A. I.; Stadnichenko, A. I.; Koscheev, S. V.; Boronin, A. I., X-ray photoelectron spectroscopy study of Pd oxidation by RF discharge in oxygen. *Applied Surface Science* **2009,** *255* (22), 9248-9254.
57. Joska, L.; Marek, M.; Leitner, J., The mechanism of corrosion of palladium–silver binary alloys in artificial saliva. *Biomaterials* **2005,** *26* (14), 1605-1611.
58. Stotz, H.; Maier, L.; Boubnov, A.; Gremminger, A. T.; Grunwaldt, J. D.; Deutschmann, O., Surface reaction kinetics of methane oxidation over PdO. *Journal of Catalysis* **2019,** *370*, 152-175.
59. Tsukada, C.; Ogawa, S.; Niwa, H.; Nomoto, T.; Kutluk, G.; Namatame, H.; Taniguchi, M.; Yagi, S., Morphological and spectroscopic studies on enlargement of Pd nanoparticle in l-cysteine aqueous solution by AFM and XPS. *Applied Surface Science* **2013,** *267*, 48-52.
60. Gladys, M. J.; El Zein, A. A.; Mikkelsen, A.; Andersen, J. N.; Held, G., Chemical composition and reactivity of water on clean and oxygen-covered Pd{111}. *Surface Science* **2008,** *602* (22), 3540-3549.
61. Khudorozhkov, A. K.; Chetyrin, I. A.; Bukhtiyarov, A. V.; Prosvirin, I. P.; Bukhtiyarov, V. I., Propane Oxidation Over Pd/Al_2O_3: Kinetic and In Situ XPS Study. *Topics in Catalysis* **2017,** *60* (1), 190-197.
62. Su, Y.-Q.; Liu, J.-X.; Filot, I. A. W.; Zhang, L.; Hensen, E. J. M., Highly Active and Stable CH_4 Oxidation by Substitution of Ce^{4+} by Two Pd^{2+} Ions in CeO_2(111). *ACS Catal.* **2018,** *8* (7), 6552-6559.
63. Hellman, A.; Resta, A.; Martin, N. M.; Gustafson, J.; Trinchero, A.; Carlsson, P. A.; Balmes, O.; Felici, R.; van Rijn, R.; Frenken, J. W. M.; Andersen, J. N.; Lundgren, E.; Grönbeck, H., The Active Phase of Palladium during Methane Oxidation. *The Journal of Physical Chemistry Letters* **2012,** *3* (6), 678-682.
64. Rogal, J.; Reuter, K.; Scheffler, M., Thermodynamic stability of PdO surfaces. *Physical Review B* **2004,** *69* (7), 075421.
65. Westerström, R.; Messing, M. E.; Blomberg, S.; Hellman, A.; Grönbeck, H.; Gustafson, J.; Martin, N. M.; Balmes, O.; van Rijn, R.; Andersen, J. N.; Deppert, K.; Bluhm, H.; Liu, Z.; Grass, M. E.; Hävecker, M.; Lundgren, E., Oxidation and reduction of Pd(100) and aerosol-deposited Pd nanoparticles. *Physical Review B* **2011,** *83* (11), 115440.
66. Wu, Y.; Chen, J.; Hu, W.; Zhao, K.; Qu, P.; Shen, P.; Zhao, M.; Zhong, L.; Chen, Y., Phase transformation and oxygen vacancies in Pd/ZrO_2 for complete methane oxidation under lean conditions. *Journal of Catalysis* **2019,** *377*, 565-576.
67. Wolf, M. M.; Zhu, H.; Green, W. H.; Jackson, G. S., Kinetic model for polycrystalline Pd/PdO_x in oxidation/reduction cycles. *Applied Catalysis A: General* **2003,** *244* (2), 323-340.
68. Mihai, O.; Smedler, G.; Nylén, U.; Olofsson, M.; Olsson, L., The effect of water on methane oxidation over Pd/Al_2O_3 under lean, stoichiometric and rich conditions. *Catalysis Science & Technology* **2017,** *7* (14), 3084-3096.
69. Zhu, G., Kinetics of Complete Methane Oxidation on Palladium Model Catalysts. *Worcester Polytechnic Institute* **2004,** *DOCTORAL DISSERTATION*.
70. Ciuparu, D.; Altman, E.; Pfefferle, L., Contributions of Lattice Oxygen in Methane Combustion over PdO-Based Catalysts. *Journal of Catalysis* **2001,** *203* (1), 64-74.
71. Martin, N. M.; Van den Bossche, M.; Hellman, A.; Grönbeck, H.; Hakanoglu, C.; Gustafson, J.; Blomberg, S.; Johansson, N.; Liu, Z.; Axnanda, S.; Weaver, J. F.; Lundgren, E., Intrinsic Ligand Effect Governing the Catalytic Activity of Pd Oxide Thin Films. *ACS Catal.* **2014,** *4* (10), 3330-3334.

Abstract Graphics